



Characterization a model of prostatic diseases and obstructive voiding induced by sex hormone imbalance in the Wistar and Noble rats

Yvonne Konkol^{1,2}, Heikki Vuorikoski^{2*}, Tomi Streng^{3,4}, Johanna Tuomela¹, Jenni Bernoulli²

¹Cancer Research Laboratory, FICAN West, Institute of Biomedicine, University of Turku, Turku, Finland; ²Pharmatest Services Ltd., Turku, Finland; ³Department of Biology, Laboratory of Animal Physiology, ⁴Department of Pharmacology, Drug Development and Therapeutics, Institute of Biomedicine, University of Turku, Turku, Finland

Contributions: (I) Conception and design: Y Konkol, J Bernoulli, T Streng; (II) Administrative support: H Vuorikoski, J Bernoulli; (III) Provision of study material: H Vuorikoski; (IV) Collection and assembly of data: Y Konkol; (V) Data analysis and interpretation: Y Konkol, T Streng, J Tuomela, J Bernoulli; (VI) Manuscript writing: All authors; (VII) Final approval of manuscript: All authors.

Correspondence to: Yvonne Konkol. Cancer Research Laboratory, FICAN West, Institute of Biomedicine, University of Turku, Kiinamylynkatu 10, 20520 Turku, Finland. Email: ymkonk@utu.fi.

Background: Chronic nonbacterial prostatitis associated with lower urinary tract symptoms (LUTS) is a prevalent condition in men. One potential pathophysiological factor is change in sex hormone, testosterone and estrogen, balance. Inflammation, cancer and obstructive voiding has been induced in the Noble rat strain by altering levels of sex hormones. We evaluated if imbalance of sex hormones could induce comparable diseases also in a less estrogen sensitive Wistar strain rats.

Methods: Subcutaneous testosterone (830 µg/day) and 17β-estradiol (83 µg/day) hormone pellets were used in male Wistar and Noble strain rats to induce prostatic diseases. The rats were followed for 13 and 18 weeks. Urodynamical measurements were performed at the end of the study under anesthesia. Prostates were collected for further histological analysis. A panel of cytokines were measured from collected serum samples.

Results: Noble rats exhibited stromal and glandular inflammation after 13 weeks that progressed into more severe forms after 18 weeks of hormonal treatment. CD68-positive macrophages were observed in the stromal areas and inside the inflamed acini. CD163-positive macrophages were present in the stromal compartment but absent inside inflammatory foci or prostate acini. Thirteen-week hormonal treatment in Noble rats induced obstructive voiding, which progressed to urinary retention after 18-weeks treatment. In the Wistar rats 18-week treatment was comparable to the 13-week-treated Noble rats judged by progression of prostatic inflammation, being also evident for obstructive voiding. Incidence of PIN-like lesions and carcinomas in the periurethral area in Noble rats were high (100%) but lower (57%) and with smaller lesions in Wistar rats. Serum cytokines leptin, CCL5, and VEGF concentrations showed a decrease in the hormone-treated rats compared to placebo-treated rats.

Conclusions: Prostate inflammation and obstructive voiding developed also in the Wistar rats but more slowly than in Noble rats. Male non-castrated Wistar strain rats may thus be suitable to use in studies of pathophysiology and hormone-dependent prostate inflammation and obstructive voiding.

Keywords: Disease model; estrogens; lower urinary tract symptoms (LUTS); prostatitis; testosterone

Submitted Jun 26, 2018. Accepted for publication Feb 15, 2019.

doi: 10.21037/tau.2019.02.03

View this article at: <http://dx.doi.org/10.21037/tau.2019.02.03>

* Present institution: Montisera Ltd., Raisio, Finland.

Introduction

Chronic nonbacterial prostatitis/chronic pelvic pain syndrome (CP/CPPS) is the most prevalent form of NIH category for prostate inflammation (1). Inflammation of the prostate is a common finding also in men with benign prostatic hyperplasia (BPH). BPH development has strong correlation between histological inflammation, IPSS (International Prostate Symptom Score), and prostate volume (2). Studies have also demonstrated a relationship between the degree of lower urinary tract symptoms (LUTS) and the degree of chronic inflammation (3,4), being associated with severity and progression of BPH (5). Benign enlargement of the prostate is the classical explanation of being the causal factor for developing bladder outlet obstruction (BOO) causing LUTS. Other factors than prostate enlargement may also contribute in the progression of BOO, perhaps independently of BPH, such as age-related declines in detrusor function, neurologic control of micturition, prostatic fibrosis, and smooth muscle contractility (6). Experimental models, where enlarged prostate, prostate inflammation and voiding functions can be concomitantly studied, are thus valuable tools for better understanding these conditions and their possible relationships to each other and, most importantly, to assess efficacy of new therapies.

An imbalance in sex hormones is evident during aging in men (7), emphasizing the role of excess estradiol serum levels associated with prostate size in BPH (8) and with storage and voiding symptoms (9). Experimental rodent models in both rats and mice have shown evidence that sex hormones play a significant role in chronic nonbacterial prostatitis development (10-13). Although clear causative factors explaining changes in sex hormone balance in men is lacking, increasing exposure to endocrine disruptor chemicals from various food, chemical and environmental could contribute to this process. Various chemicals possess sex hormone-like actions (14) and thus can eventually interfere with the endogenous sex hormone balance. There are not many models available for studying changes in the LUT function concomitantly with the progression of the inflammation process induced with estrogen and testosterone unbalance. Nicholson *et al.* (11) showed testosterone (T) + 17 β - estradiol (E₂)-induced voiding dysfunction and BOO in mice. In rats, the hormone-sensitive Noble strain has been used for modelling both development of chronic prostate inflammation and associated obstructive voiding (12,15). In this model, the

rats treated with high levels of T and E₂ show signs of obstructive voiding concomitant with chronic prostatic inflammation. In addition, the hormonal treatment in this strain leads to development of cancerous lesions around the prostatic ducts (16,17), thus diversifying the potential of the model for investigational purposes. Though the hormone sensitive Noble rat strain (17) has been used in hormone related studies for decades, its use is currently limited due to decreased availability of this strain by commercial laboratory animal suppliers. More commonly used rat strains should be available for studying the effects of imbalance of sex hormones on LUT.

It is shown that castrated Wistar rats develop prostate inflammation after hormone exposure (13,18,19). Moreover, treating aged Wistar rats with estrogen induces prostate inflammation with 100% incidence (20). In the present study, we evaluated if the non-castrated, namely hormonally less sensitive Wistar rats at young adult age with chronic testosterone and estrogen exposure, leads to development of prostate inflammation and cancer, and especially, whether obstructive voiding is associated in the condition. Finally, we compared results from the Wistar rat strain with the Noble rat strain, to investigate possible differences in the degree of treatment effects on LUT in these strains. In addition, various serum cytokines in serum were evaluated for potential biomarkers. The presence of macrophages in the inflamed prostate was also assessed, since they are commonly found associated in prostate inflammation and in (2) and prostate cancer (21).

Methods

Experimental design

Adult (11–12 weeks old, 340 \pm 20 g) male Wistar rats (Harlan Laboratories Inc., The Netherlands) and 9–14 weeks old (308 \pm 20 g) Noble rats (Charles River (Raleigh, NC, USA) were used. All animals were housed pairwise under a 12-h light-dark cycle. The animals had free access to soy-free rodent pellets (2016 global 16% protein rodent diet, Harlan/ Envigo, Huntingdon, UK) and tap water *ad libitum*. Animal experiment was complying the EU Directive 2010/63/EU, and the study protocol (10428/Ym23 STH697A and STH077A) was approved by the National Animal Experiment Board of Finland. The animals were stratified evenly into treatment groups based on body weights.

In order to treat the animals chronically, subcutaneous

testosterone (T, 50 mg for 60-day release pellets, calculated daily release 830 µg), and 17β- estradiol (E₂, 5 mg for 60-day release pellets, calculated daily release 83 µg) were used. The use of corresponding hormone concentrations, resulting to a hyperandrogenic state with decreased T-to-E₂ ratio, has been shown to induce both prostate inflammation and obstructive voiding in Noble-rats (12). Corresponding placebo hormone pellets (IRA, FL, USA) were used for the placebo treated control groups. The pellets were implanted subcutaneously over the scapular area under anesthesia (3% isoflurane, 200 mL/min, Piramal Healthcare Ltd, UK). The pellets were replaced with identical new ones either twice (at study weeks 6 and 13 for the 18-week treatment groups) or once (at study week 6 for the 13-week treatment groups). Since the progression time of prostate inflammation in the Wistar rat strain was uncertain using these hormonal treatments, two of the Wistar animals were terminated at the study week 13 to assess the inflammation stage of the prostate. Due to low observed inflammation, the treatment period for the Wistar rats was extended to 18 weeks. Thus, following groups were in the study: Noble T+E₂-group and placebo-group with 13 weeks treatment period; Noble T+E₂-group and placebo-group with 18 weeks treatment period, and Wistar T+E₂-group and placebo-group with 18 weeks treatment period.

Urodynamic measurements

For evaluating possible changes in micturition pattern indicating obstructive voiding, urodynamic measurements were performed as described previously (22) at the end of each study period. Briefly, under anesthesia, an incision was made to the lower abdomen of the rats and a 20G i.v. cannula was inserted into the bladder for infusion of warm (+37 °C) saline evoking the micturition and for bladder pressure recordings. Urine flow rate was measured with an ultrasonic flow probe from distal part of the urethra. The pressure and urine flow signals were transferred to a Biopac-system and continuous recording was made with Acq Knowledge 3.5.3 software (Biopac Systems Inc., Santa Barbara, CA, USA). At the end of the measurements the animals were sacrificed under anesthesia using CO₂ suffocation and neck dislocation. The bladders, prostate-urethra complex (including dorsal, lateral and ventral prostate lobes and the underlying urethra part inside the prostate), and pituitary glands were weighted and collected. The prostate samples were fixed with 10% neutral buffered formalin for 24 hours and stored thereafter in 70% ethanol

for further analysis.

Histology

For histopathological evaluation of the prostate, the collected prostate-urethra complexes were embedded in paraffin, cut at 5 µm thickness and placed on glass slides. The sections were deparaffinized with xylene and decreasing ethanol solutions (100%, 96% and 70%) and rehydrated with distilled water. For assessment of inflammation and cancerous areas sections were stained with hematoxylin-eosin, dehydrated and mounted. Three representative serial sections of each animal's dorsolateral prostate were viewed for the assessment. The number of inflamed acini were quantified from the dorsolateral prostate lobes. Presence of prostatic intraepithelial neoplasia (PIN)-like lesions and cancerous areas (adenocarcinoma) was assessed in the rat according as previously published (23). Briefly, PIN-like lesions were defined as focal areas of hyperplastic epithelium displaying distinct variation in size, shape, and staining properties of cells and nuclei. Observed cancerous areas were identified as prostatic adenocarcinomas and were locally invasive lesions characterized by abnormalities in glandular architecture and cytological atypia. All assessment was performed blinded to treatment groups.

Macrophages were assessed from 13- and 18-week treated Noble rats. Immunohistochemical staining with CD68 and CD163 antibodies was used to detect macrophages present in the prostate tissue. The staining procedure was performed using automatized Thermo Scientific™ Lab Vision™ Autostainer (Fisher Scientific, New Hampshire, USA) platform performed by BioSiteHisto Ltd, Tampere, Finland. Briefly, after deparaffinization and dehydration procedures, antigen retrieval was performed in pretreatment module in Tris-EDTA pH9 buffer (20 min in +98 °C). The primary antibodies CD68 (mouse monoclonal antibody clone ED1, ab3163, dilution 1:250); and CD163 (rabbit monoclonal antibody clone EPR19518, ab182422, dilution 1:500, both Abcam, Cambridge, UK) were incubated for 30 min. Endogenase peroxidase activity was blocked with 3% H₂O₂, 10 min. Anti-mouse and anti-rabbit HRP detection polymers (Nordic Biosite, Täby) were incubated for 30 min. Diaminobenzidine (DAB) chromogen (High contrast DAB, Nordic Biosite, Täby) was used for visualization of the antibody complex. The slides were then counterstained with 1:5 diluted Mayer's hematoxylin, dehydrated and mounted with permanent mounting media.

For negative controls similar procedure was performed without the primary antibody.

Serum analysis of cytokines

A panel of cytokines was assessed from serum samples of the Wistar rat strain from both groups (T+E₂ and placebo group) at two different time points: at week 13 and week 18 prior to termination. For obtaining serum samples, blood samples were collected from the tail vein, centrifuged for 10 min, serum was collected and stored at -70 °C for further analysis. Cytokines were measured using ELISA method-based Milliplex[®] immunoassay biomarker panel (Merck Millipore, Merck KGaA, Darmstadt, Germany) Following 23 different biomarkers were measured from serum samples: Eotaxin, GM-CSF, G-CSF IL-1A, MCP-1, Leptin, MIP-1A, IL-4, IL-1B, IL-2 IL-6, IL-13, IL-10, IL-12p70, IL-5, IFN γ , IL-17,IL-18, IP-10, GRO-KC, CCL5, TNF α , and VEGF. Cytokine concentrations were measured from two replicate samples.

Statistical analysis

Statistical analysis was performed using GraphPad Prism 7.01. (GraphPad Software Inc., La Jolla, CA, USA). Statistical comparisons were performed between each T+E₂-group with its placebo control group. Data was checked for normality using Shapiro-Wilk test. The cytokine data was analyzed using two-way repeated measures ANOVA with Sidak's multiple comparisons test and the differences were tested between time points inside each treatment group (13- vs. 18-week) and between treatments in both time points (T+E₂ vs. placebo-treatment) separately at both time points (13- and 18-week). All other normally distributed data was analyzed using two-tailed t-test, or non-parametric Mann-Whitney U test was used as a *post hoc* test. P values <0.05 were considered statistically significant.

Results

Animal and organ weights in the Wistar and Noble strain rats

The placebo-treated animal weights increased in all treatment groups. On the contrary, the body weights of all hormone-treated animals decreased at the end of each treatment period, compared to the start weight (week 0). The prostate and pituitary gland weights were significantly

increased in all three T+E₂-treated groups compared to the corresponding placebo-groups. The bladder weights of both the 13- and 18-week T+E₂-treated Noble strains were significantly increased compared to the control groups. In contrast, the bladder weights of the T+E₂-treated Wistar rats were not significantly increased (*Table 1*). Comparisons were performed using absolute organ values.

Prostate cancer and inflammation in the Wistar and Noble strain rats

After 13 weeks of hormonal treatment only sparse inflammation was evident in the Wistar rats, thus the study period for the Wistar was continued up to 18 weeks. The inflammation in the prostate was most extent in the 18-week T+E₂-treated Noble group, seen as higher number of inflamed prostate acini and extent stromal and periglandular inflammation. In contrast, the 13-week Noble rats and the 18-week Wistar rats showed less inflamed acini and mild stromal inflammation was observed (*Table 1*). Prostate inflammation in the Wistar rats after 18 weeks was evident as glandular, perivascular and stromal inflammatory sites compared with placebo-treated healthy rats (*Figure 1A,B,C,D*). Similar morphology was seen in the T+E₂-treated Noble groups (data not shown), which was consistent with earlier findings (24). Adenocarcinomas and PIN-like lesions around the prostatic ducts in the periurethral area were present in both Noble groups in all hormone-treated animals and was in accordance to previous data (16). Only four animals out of seven showed cancer areas in the periurethral area in Wistar rats (*Table 1*). These lesions were smaller (qualitative evaluation) compared to the Noble rats. Representative histopathological images from hormone-treated Wistar rats compared to placebo treated animals are shown in *Figure 1E,F*.

Urodynamic parameters in the Wistar and Noble strain rats

During the urodynamical measurements of the 18-week T+E₂ Noble rats it was evident that these animals exhibited severe urinary obstruction making it impossible to execute urodynamical recording under anesthesia. Thus, urodynamic data was collected and analyzed from the 18-week Wistars and the 13-week Noble rats only. The basal bladder pressure, i.e., bladder pressure during the micturition phases, and the mean and maximal micturition bladder pressure were significantly elevated compared

Table 1 Comparison of different parameters investigated

Parameters	Noble 13-week			Noble 18-week			Wistar 18-week		
	Placebo	T+E ₂	P	Placebo	T+E ₂	P	Placebo	T+E ₂	P
Body weight change (g)	60.8 ±7.2	-35.2±4.5	<0.0001 (T)	67.7±6.5	-36.6±6.3	<0.0001 (T)	143.0±6.9	-29.6±3.2	<0.0001 (T)
Pituitary weight (absolute values) (10 ⁻² g)	1.1±0.04	3.2±0.3	<0.0001 (T)	1.1±0.05	5.1±0.3	<0.0001 (T)	1.2±0.06	4.8±0.8	0.0002 (T)
Prostate weight (absolute values) (10 ⁻¹ g)	11.1±0.4	19.9±0.5	<0.0001 (T)	12.0±0.7	19.7±0.4	<0.0001 (T)	14.1±0.9	24.9±1.2	<0.0001 (T)
Bladder weight (absolute values) (10 ⁻¹ g)	1.4 ±0.05	2.0±0.06	<0.0001 (T)	1.5±0.04	2.1±0.1	0.0073 (T)	1.3±0.04	1.4±0.1	NS (T)
Number of Inflamed prostate acini	0	15±2.4		0	32±6.4		0	18±3.8	
Cancer incidence (% of total)	0	100		0	100		0	57	
Urodynamical parameters									
Basal bladder pressure (cmH ₂ O)	4.4±0.9	4.4±1.1	NS (M)	NM	NM		6.2±0.8	15.9±2.2	0.0013 (T)
Max bladder pressure (cmH ₂ O)	59.0±2.1	60.4±2.3	NS (T)	NM	NM		42.3±1.4	55.5±2.5	0.0006 (T)
Mean bladder pressure (cmH ₂ O)	42.0±1.9	44.2±1.1	NS (T)	NM	NM		32.5±1.9	46.0±2.4	0.004 (M)
Max. flow rate (mL/min)	32.5±8.6	17.9±4.4	NS (T)	NM	NM		23.2±7.3	16.5±4.3	NS (T)
Mean flow rate (mL/min)	5.0±1.2	3.5±0.7	NS (T)	NM	NM		4.4±1.3	2.7±0.5	NS (T)
Micturition time (s)	8.7±1.3	12.0±1.9	NS (M)	NM	NM		13.4±3.4	25.0±3.0	0.038 (M)
Micturition interval (min)	1.9±0.3	2.5±0.4	NS (T)	NM	NM		2.2±0.3	2.8±0.2	NS (T)
Bladder capacity (mL)	0.7±0.07	1.0±0.10	0.012 (T)	NM	NM		0.8±0.07	1.4±0.26	0.029 (M)
Residual urine volume (mL)	0.32±0.06	0.58±0.09	0.030 (T)	NM	NM		0.48±0.06	1.08±0.29	0.053 (M)

Upper values in the rows are mean and SEM values for each parameter. Lower values in each row are P values from pairwise comparisons against each placebo-groups. NS, not significantly different. P values >0.05 but <0.1 are shown also as exact values. Statistical analysis between each T+E₂-group compared to their placebo-groups was performed either with *t*-test (T) or Mann-Whitney test (M). NM, not measured. Animal and organ weights and urodynamical parameters: Wistar groups n=7; Noble groups n=10; histological parameters: Noble 13-week group n=8, Noble 18-week group n=5, Wistar 18-week group n=7.

to their placebo groups in the Wistar rats but not in the Noble rats. Maximal and average mean urine flow rates during the micturition phase were reduced in both strains but the differences were not statistically significant, due to high variation between the interindividual animals. The micturition times were significantly elevated in the Wistar-T+E₂ group compared to the placebo-group, and in the T+E₂ Noble group a similar statistical trend was observed. The bladder capacities and residual urine volumes after voiding in both strains were increased in the T+E₂-group

compared to their placebo treated control groups. Increase in the micturition intervals of the T+E₂-treated groups in both strains was not statistically significant (*Table 1*).

Presence of CD68-positive and CD163-positive macrophages in the Noble rat prostate

Macrophages were assessed from 13- and 18-week treated Noble rats to evaluate the macrophage infiltration differences between the timepoints, since inflammation

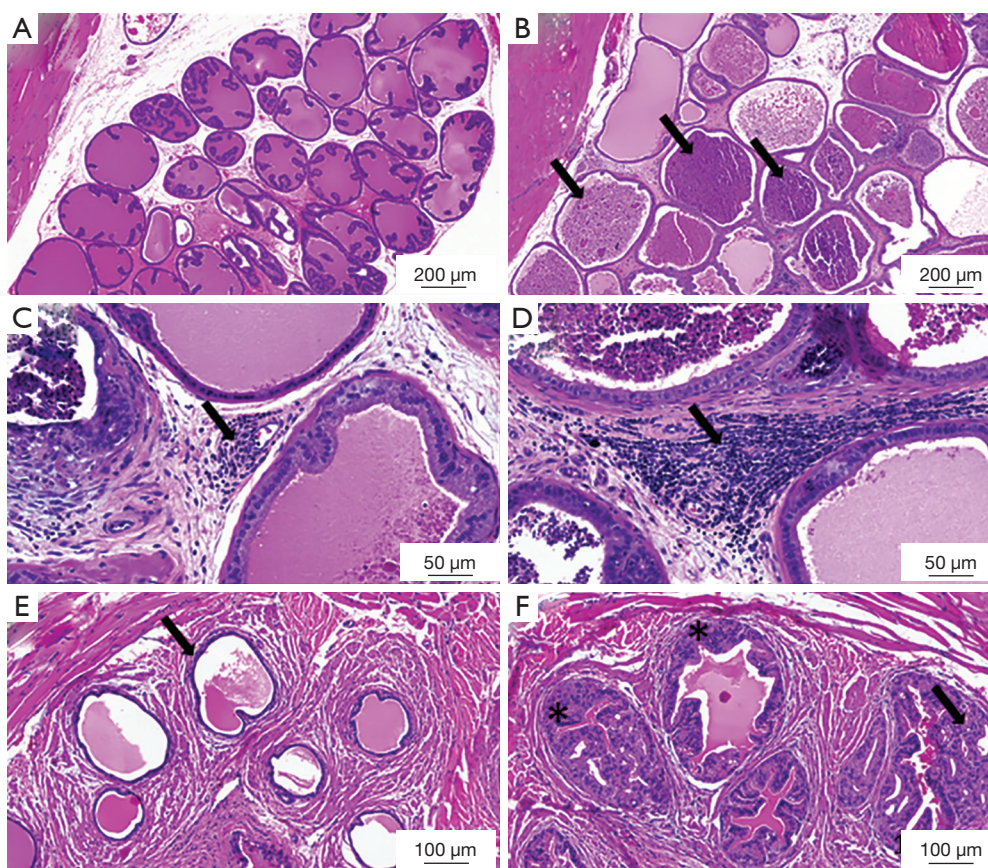


Figure 1 Chronic inflammation and cancerous areas in the Wistar rat prostates. (A) Representative image (50× magnification) of the lateral prostate lobe from a healthy placebo-animal in the 18-week Wistar group; (B) inflamed prostate acini (arrows showing examples) in the lateral prostate lobe after 18-week hormone treatment in the Wistar rat (50× magnification); (C) inflammatory infiltrates in the Wistar T+E₂-treated rats are evident around capillaries (arrow) and (D) in the stroma (arrow) between prostate lobes (250× magnification); (E) representative image of the periurethral area from a healthy Wistar rat where the prostatic ducts with normal epithelial layer are seen (arrow) (150× magnification); (F) periurethral area of a T+E₂-treated Wistar rat showing some small adenocarcinoma area (arrow) and PIN-like lesions (stars) around the prostatic ducts (150× magnification).

severity increased with study course. Only few CD68- or CD163-positive macrophages were present in the connective tissue space around the prostatic acini in the placebo-treated groups (Figure 2A,B). Hormone treatment and resultant inflammation increased presence of both CD68- and CD163-positive macrophages intensely. CD68-positive cells were present in the prostate acini, stroma and inside inflammation infiltrate areas (Figure 2C). In contrast, CD163-positive macrophages were present strictly in the prostate stromal compartment but not inside the inflammatory foci areas (Figure 2D) In the periurethral space similarly only few CD68- or CD163-positive cells were present in the healthy tissue around the prostatic ducts of the placebo-treated rats (Figure 2E,F).

In contrast, CD68-positive cells were abundantly visible in the connective tissue around the cancerous area and some inside the cancerous region in the periurethral space in the hormone-treated rats (Figure 2G). In the hormone-treated rats, also CD163-positive macrophages were present in the periurethral area (Figure 2H). Qualitatively no differences in abundance of macrophages was observed between the 13- and 18-week-treated Noble rats.

Serum cytokine concentrations

Hardly any inflammation in the prostate was evident in the Wistar rats at timepoint 13. Thus, cytokines/chemokines were measured from serum samples of the Wistar

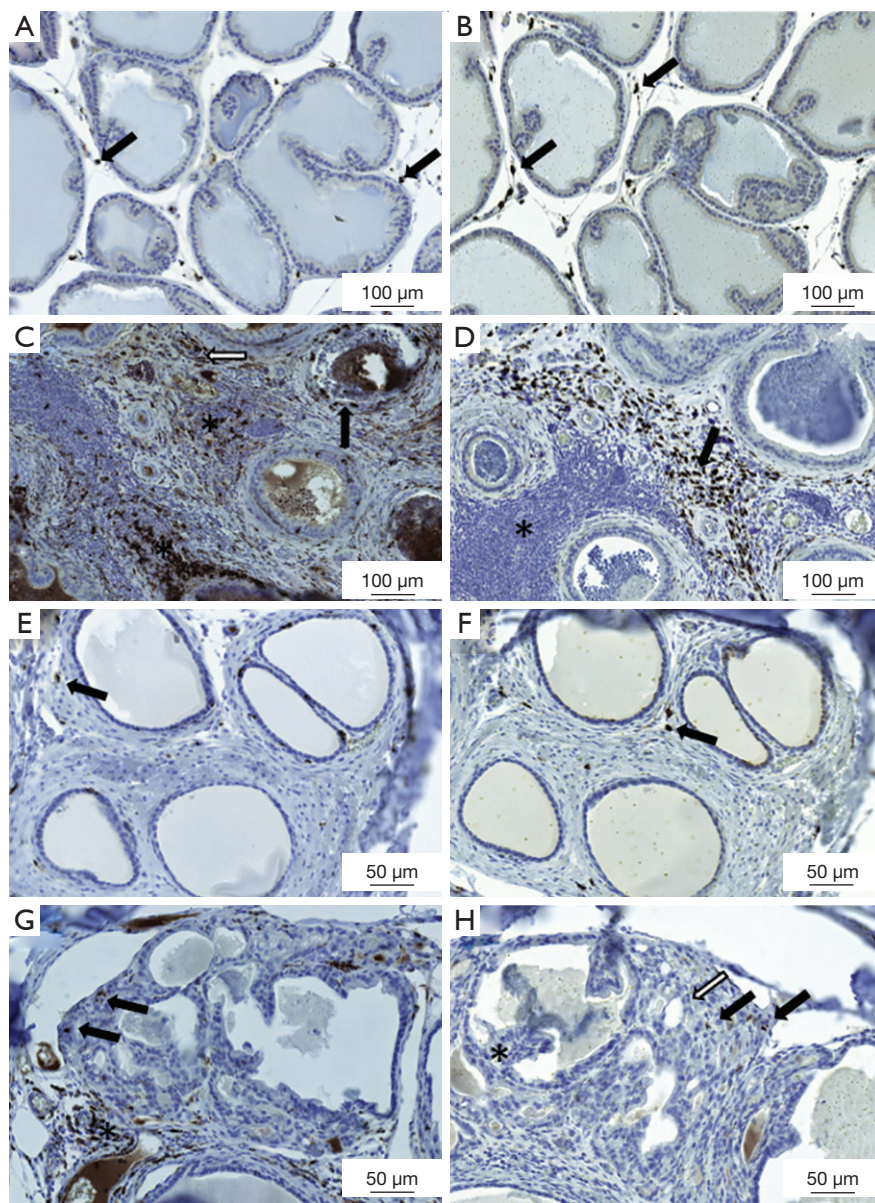


Figure 2 Presence of macrophages in the prostate and periurethral area. (A-D) Representative figures demonstrating presence of CD68- and CD163-positive macrophages in the lateral prostate lobe of the 18-week treated Noble strain. Only few (A) CD68- or (B) CD163-positive macrophages are present in the placebo rat (arrows); (C) presence of CD68-positive cells in the prostate acini (black arrow), stroma (white arrow) and inside the inflammation infiltrate areas (stars) in the lateral prostate lobe from a hormone-treated rat; (D) representative figure from a hormone-treated rat with extent CD163-positive cells in the prostatic stroma (arrow) but not in the inflammation infiltrate areas (star) of the lateral prostate lobe; (E-H) CD68- and CD163-positive macrophage staining in the periurethral area; (E) only few CD68-positive cells or (F) CD163-positive are seen in the healthy prostate tissue around the prostatic ducts (arrows) in the placebo-treated rat; (G) cancerous areas in the periurethral space around the prostatic ducts with infiltration of CD68-positive macrophages in the connective tissue (star) around the cancerous area and few cells inside the cancerous region in the hormone-treated rat (arrows); (H) hormone-treated rat with PIN-like lesions (star) and cancerous area (white arrow) in the periurethral space around the prostatic ducts and only few CD163-positive cells visible around that area (black arrows). (A-D) 150× magnification, (E-H) 200× magnification.

Table 2 Cytokine and chemokine concentrations in serum of the Wistar rat

Cytokine/ chemokine	Placebo timepoint 13-week	T+E ₂ timepoint 13-week	Placebo timepoint 18-week	T+E ₂ timepoint 18-week	Significance (P) between timepoints within treatments	Significance (P) between treatments
Leptin (ng/mL)	33.6±6.2	14.6±3.4	35.7±4.7	11.5±2.5	NS	0.014 (13-week), 0.0017 (18-week)
IL-1A (pg/mL)	506±197	183±97	207±86	103±103	NS	NS
IL-2 (pg/mL)	25±11	76±42	29±14	23±12	NS	NS
IL-4 (pg/mL)	159±54	79±39	143±43	125±41	NS	NS
IL-10 (pg/mL)	156±63	10±10	138±54	0±0	NS	NS (P=0.062, 13 weeks), NS (P=0.081, 18 weeks)
IL-12p70 (pg/mL)	174±25	163±15	156±20	191±21	NS	NS
IL-18 (pg/mL)	425±104	394±94	179±60	74±35	NS	NS
CCL5 (ng/mL)	82.9±9.3	16.9±3.3	83.1±9.1	11.8±5.8	NS	<0.0001 (13 weeks), <0.0001 (18 weeks)
Eotaxin (pg/mL)	246±47	211±7	228±19	220±22	NS	NS
GRO-KC (pg/mL)	756±130	518±165	704±109	406±106	NS	NS
MCP-1 (pg/mL)	593±55	557±69	612±54	567±54	NS	NS
VEGF (pg/mL)	240±11	210±10	235±7	201±11	NS	NS (P=0.085, 13 weeks), 0.039 (18 weeks)

Concentration values are represented as mean and SEM (as ng/mL for Leptin and CCL5, others as pg/mL). NS, non-significant. P values >0.05 but <0.1 are shown also as exact values. Samples with concentrations <0.24 pg/mL were under the detection limit and considered as 0 ng/mL for statistical comparisons. Placebo: n=11, T+E₂: n=9.

18-week rat groups at two different time points, at 13 and 18 weeks, to evaluate, if there is a gradual change in time of cytokines present in the blood indicating progression of the inflammation. Eleven of them (GM-CSF, G-CSF, MIP-1A, TNF- α , IL-1B, IL-6, IL-13, IL-5, IL-17, IP-10, IFN γ) out of 23 were at concentrations under the detection limit (24 pg/mL) in both treatment groups and in both time points (data from these not shown in the table). Results from the other cytokines are listed in the *Table 2*. Inside each treatment groups, there was no change in the concentrations between the timepoints 13 and 18 weeks in any cytokines measured in neither T+E₂- or placebo-group. Instead, there was a statistically significant reduction in leptin and CCL5 in the T+E₂-group compared to the placebo-group in both timepoints. Similarly, there was some decrease in concentrations of IL-10 and VEGF in the T+E₂-group compared to the placebo-group (*Table 2*).

Discussion

Long term estrogen treatment is known to induce chronic prostate inflammation in rodents (10-13). In addition to effects of estrogen on the prostate, studies suggest that estrogens influence function of the LUT as well. Both estrogenisation of neonatal mice (25) and aromatase over expression in transgenic mice (26) leads to altered voiding patterns resembling obstructive voiding. In addition, a study by Streng *et al.* (27) suggests that only high doses but not low doses of estrogens are able to induce voiding dysfunction in male mice. In the rats, estrogen treatment alone does not appear to be sufficient to induce voiding symptoms associated with prostate inflammation (28). Combined T+E₂ treatment on the other hand, has been shown to be an effective approach to induce LUTS as shown in studies in mice (11) and in the Noble strain rats (12,15). New animal models would contribute and

significantly support preclinical assessment of novel therapies targeting chronic prostate inflammation and LUTS. We therefore evaluated the Wistar rat strain for obstructive voiding associated with hormonally induced chronic prostate inflammation and compared the results to the Noble strain.

The degree of inflammation in both Noble strain groups (13- and 18-week-treated) were consistent with previous published data (24). Inflammation was evident in both prostatic acini and in the prostatic stromal space in both strains. The degree of prostate inflammation in the 18-week treated Wistar strain was similar with the 13-week treated Noble strain, indicating less sensitivity of the Wistar strain to hormonal exposure. Less sensitivity to the hormonal treatment was also evident as lower cancer incidence and fewer adenocarcinoma areas in the Wistar strain. On the other hand, the weights of the pituitary glands (which is a consistent indicator of estrogen effect in this model), and the prostate sizes (which is a consistent indicator of testosterone effect in this model) were nevertheless similar in both 18-week treated Wistars and Nobles indicating that the level of hormone exposures was similar. Thus, it can be concluded that the Wistar strain is suitable as a model for chronic prostate inflammation. For reason that remains unclear, prostate cancer in the periurethral area does not develop in Wistar rats as in the Noble rat strain. Thus, this Wistar animal model is not an optimal choice for cancer research but highlights its usefulness for investigating therapy options for obstructive voiding.

One method to measure obstructive voiding is the pressure/flow evaluation, where high detrusor pressure associated with low urinary flow rate may occur, but also other combinations may indicate the possibility of detrusor failure, such as low detrusor pressure associated with low urinary flow rates (29). Our results show that the basal bladder pressure was not altered in the Noble strain, whereas in the Wistar strain it was significantly elevated. Obstruction was evident, and seen as increase of micturition times, bladder capacity and residual urine volumes. This suggests that the bladder's ability of emptying itself from urine during voiding was impaired. In humans, a normal urine flow rate does not preclude the possibility of obstruction, and therefore concomitant analysis of flow rates and residual volumes are used when interpreting the data (29).

In the Wistar strain rats, the bladder weights were slightly but not significantly increased in the hormone-treated rats, unlike in both Noble strains (13- and 18-

week treated). It is known that the bladder enlarges due to BOO. Enlargement compensates the increased tension of the urethra and enables emptying of the bladder (30). Experimental studies have demonstrated that the bladder undergoes three sequential stages (hypertrophy, compensation, and decompensation) during the steps of BOO progression (31). Surgical induction of BOO has demonstrated immediate increases in urethral resistance to urine flow, initiating an increase in bladder mass. After that the bladder enters the compensated stage: the bladder mass stabilizes, and the bladder pressure either remains normal or increases to greater than control value, and the bladder's ability to empty remains near to normal. Thereafter, bladder function destabilizes and enters the decompensated stage, which is characterized by further increase in bladder mass, progressive decreases in both phasic and tonic bladder pressure and progressive loss in the bladder's ability to empty (31). Taken together, obstruction is evident in our results, but with a difference that in the Wistar rats the progression of decompensation stage is probably not as far progressed as in the Noble rats: the bladder weights were not significantly increased and there is still increased bladder pressure remaining resisting the increased tension of the urethra.

Prostate sizes were similarly enlarged in all studied hormone-treated groups. Despite similar prostate weights in the 18-week-treated Noble rats compared to the 13-week Noble rats and the 18-week Wistar rats, the obstruction in this group was extreme and thus different. Our results support the finding that the prostate size does not directly correlate with the severity of obstructive dysfunction as what has been observed in men with BPH (32). Moreover, our results lend support to the idea that inflammation in the prostate contributes to the onset of LUTS in histologic BPH (33). This is because of degree of inflammation and the obstruction were generally similar in both 13-week treated Nobles rats and 18-week treated Wistar rats. In contrast, in the 18-week treated Noble rats, more severe degree of inflammation and more severe obstruction was evident. Support of the association of prostate inflammation progression with development of obstructive voiding has been provided also in the previous study by Bernoulli *et al.* (15).

We evaluated the presence of macrophages in this hormonal model, since they are of high interest in the context of immunotherapy development. Macrophages are antigen presenting cells that play a role in the first step of the innate inflammatory response. In this model

both CD68- and CD163-positive macrophages were abundantly present in the stroma of the inflamed regions in the prostate. Both markers are being used to identify macrophages in tissue: CD68 is considered as a general marker for all types of macrophages and CD163 is abundantly referred as a marker for M2-type polarized macrophages (with regulatory functions in tissue repair and wound healing), although CD163 alone cannot be considered a reliable M2-type marker when used on its own (34). Both macrophage markers are being used frequently for identification in immunohistochemistry. It is known that the presence of macrophages in the inflamed tissue is a common finding in prostate inflammation: Robert *et al.* (2) showed presence of CD163-positive macrophages in 82% of specimens from BPH patients. Interestingly, CD163-positive macrophages have been found to correlate also with pain and discomfort symptoms in patients with prostate inflammation (35). Macrophage infiltration into prostate tissue has been reported to correlate with tumor progression. In most tumors the infiltrated macrophages are considered to be toward M2 phenotype, which provides an immunosuppressive microenvironment for tumor growth and correlates with poor prognosis (36). However, increased numbers of CD68-positive-macrophages are found in specimens from high grade PIN and prostate cancer lesions compared with benign prostate specimens (21). We discovered that only some CD68-, but not CD163-positive-macrophages, were present in the cancerous areas in this hormonal model used. We did not observe any CD163-positive cells at the adenocarcinoma site. It could be speculated that the high estrogen used in this model is involved in inhibiting the recruitment of CD163-positive macrophages to the cancerous areas, since it has been shown that estrogen can reduce macrophage recruitment in estrogen receptor (ER α)-positive cancer associated fibroblasts (37). In addition, estrogen has shown to influence differentiation of macrophages (38). It is possible, that estrogens used in this model has a major influence on macrophage infiltration into tumors sites.

Prostatic inflammation in men has shown to elevate inflammatory cytokine levels and is associated with symptom severity in patients with CP/CPHS and BPH (39). In humans, inflammatory biomarkers from patients with prostatitis are mainly measured from seminal plasma, but certain markers have been shown to be elevated also measured from serum samples in preclinical models.

For instance, increased serum levels of TNF- α has been measured in a carrageenan-induced rat model (40) and increased IL-1 β levels has been shown to be elevated in a rat autoimmune model for chronic prostatitis (41). In a short term (30 days) estradiol-induced prostate inflammation model serum cytokines TNF- α and IL-6 was shown to be elevated in Wistar rats (42). Finding a reliable inflammatory biomarker, ideally measurable from blood samples, would help following the progression of the inflammation in preclinical models. Our results showed no changes in measured cytokine and chemokine concentrations in the hormone-treated rat serums during the progression of inflammation in the prostate. Therefore, they are not suitable biomarkers for inflammation in this model. In addition, few inflammatory biomarkers (CCL5, VEGF and leptin) showed a decrease, rather than an increase, in serum concentrations in the hormone-treated rats, most probably due to high estrogen or testosterone influence. Estrogen has shown inhibitory actions on CCL5 (37). Regarding decrease of VEGF, it has been shown that both estrogen and testosterone increases VEGF expression levels in prostate tissue (43), however, also a decreasing expression effect on VEGF levels have been observed with an ER β 1 agonist (44). A dual effect of sex hormones is evident also on leptin expression: estradiol has an increasing effect while testosterone have a suppressive effect on leptin levels (45). Thus, it seems that the role of sex hormones on different inflammatory biomarkers is rather complex and unrevealed and needs to be clarified further.

In summary, the Wistar rat is a suitable strain for modelling chronic prostate inflammation and obstructive voiding. The Wistar strain is not, however, the optimal model for preclinical cancer studies due to lower cancer incidence and smaller cancer acini areas. The Wistar rat strain less sensitive to hormonal exposure compared with the Noble rat strain. Therefore, the corresponding prostate inflammation and obstructive voiding is achieved using longer hormonal exposure times. The effects of estrogen on LUT are complex and can have unpredicted effects on biomarkers being investigated. Thus, characterization of experimental models is important to understand the potential and limitations of the models for specific targeting. The use of the Wistar strain enables investigating the relationship of sex hormones on prostatic inflammation and associated obstructive voiding and most importantly, for the preclinical assessment of novel therapeutics targeting voiding disorders.

Acknowledgements

We warmly thank Mrs. Natalia Habilainen-Kirillov for her skillful technical assistance on animal handling and preparing histological prostate sections. The measurements of cytokines were performed by Millipore BioPharma Services, Oxfordshire, UK and immunohistological stainings by BioSiteHisto, Tampere, Finland. Prof. Pirkko Härkönen and Dr. Katri Selander are appreciated for valuable comments of the manuscript text.

Funding: This work was supported by Finnish Funding Agency for Technology and Innovation (40257/05); Turku University foundation (to Y Konkol) and Faculty of Medicine (Drug Research Doctoral Program), University of Turku (to Y Konkol).

Footnote

Conflicts of Interest: Y Konkol, H Vuorikoski and J Bernoulli were employees at Pharmatest Services Ltd at the time of the study. The other authors have no conflicts of interest to declare.

Ethical Statement: Animal experiment was complying the EU Directive 2010/63/EU, and the study protocol (10428/Ym23 STH697A and STH077A) was approved by the National Animal Experiment Board of Finland.

References

- Habermacher GM, Chason JT, Schaeffer AJ. Prostatitis/Chronic Pelvic Pain Syndrome. *Annual Review of Medicine* 2006;57:195-206.
- Robert G, Descazeaud A, Nicolaiew N, et al. Inflammation in Benign Prostatic Hyperplasia : A 282 Patients ' Immunohistochemical Analysis. *Prostate* 2009;69:1774-80.
- Mizuno T, Hiramatsu I, Aoki Y, et al. Relation between histological prostatitis and lower urinary tract symptoms and erectile function. *Prostate Int* 2017;5:119-23.
- Nickel JC, Roehrborn CG, Leary MP, et al. The Relationship between Prostate Inflammation and Lower Urinary Tract Symptoms : Examination of Baseline Data from the REDUCE Trial. *Eur Urol* 2008;54:1379-84.
- Nickel JC, Roehrborn CG, Castro-santamaria R, et al. Chronic Prostate Inflammation is Associated with Severity and Progression of Benign Prostatic Hyperplasia , Lower Urinary Tract Symptoms and Risk of Acute Urinary Retention. *J Urol* 2016;196:1493-8.
- Wynder JL, Nicholson TM, DeFranco DB, et al. Estrogens and Male Lower Urinary Tract Dysfunction. *Curr Urol Rep* 2015;16:61.
- Srilatha B, Adaikan PG. Endocrine milieu and erectile dysfunction: Is oestradiol-testosterone imbalance, a risk factor in the elderly? *Asian J Androl* 2011;13:569-73.
- Roberts RO, Jacobson DJ, Rhodes T, et al. Serum Sex Hormones and Measures of Benign Prostatic Hyperplasia. *Prostate* 2004;61:124-31.
- Martin S, Lange K, Haren MT, et al. Risk Factors for Progression or Improvement of Lower Urinary Tract Symptoms in a Prospective Cohort of Men. *J Urol* 2014;191:130-7.
- Vykhovanets EV, Resnick MI, MacLennan GT, et al. Experimental rodent models of prostatitis : limitations and potential. *Prostate Cancer Prostatic Dis* 2007;10:15-29.
- Nicholson TM, Rieke EA, Marker PC, et al. Testosterone and 17 β -estradiol induce glandular prostatic growth, bladder outlet obstruction, and voiding dysfunction in male mice. *Endocrinology* 2012;153:5556-65.
- Bernoulli J, Yatkin E, Konkol Y, et al. Prostatic inflammation and obstructive voiding in the adult noble rat: Impact of the testosterone to estradiol ratio in serum. *Prostate* 2008;68:1296-306.
- Vykhovanets EV, Resnick M, Marengo S. Intraprostatic Lymphocyte Profiles in Aged Wistar Rats With Estradiol Induced Prostate Inflammation. *J Urol* 2006;175:1534-40.
- Marcoccia D, Pellegrini M, Fiocchetti M, et al. Food components and contaminants as (anti)androgenic molecules. *Genes Nutr* 2017;12:6-16.
- Bernoulli J, Yatkin E, Talvitie EM, et al. Urodynamic changes in a noble rat model for nonbacterial prostatic inflammation. *Prostate* 2007;67:888-99.
- Bernoulli J, Yatkin E, Laakso A, et al. Histopathological evidence for an association of inflammation with ductal pin-like lesions but not with ductal adenocarcinoma in the prostate of the noble rat. *Prostate* 2008;68:728-39.
- Bosland MC, Ford H, Horton L. Induction at high incidence of ductal prostate adenocarcinomas in NBL/Cr and Sprague-Dawley Hsd:SD rats treated with a combination of testosterone and estradiol-17 beta or diethylstilbestrol. *Carcinogenesis* 1995;16:1311-7.
- Wilson MJ, Woodson M, Wiehr C, et al. Matrix metalloproteinases in the pathogenesis of estradiol-induced nonbacterial prostatitis in the lateral prostate lobe

- of the Wistar rat. *Exp Mol Pathol* 2004;77:7-17.
19. Robinette CL. Sex-hormone-induced inflammation and fibromuscular proliferation in the rat lateral prostate. *Prostate* 1988;12:271-86.
 20. Naslund MJ, Strandberg JD, Coffey DS. The role of androgens and estrogens in the pathogenesis of experimental nonbacterial prostatitis. *J Urol* 1988;140:1049-53.
 21. Fang LY, Izumi K, Lai KP, et al. Infiltrating macrophages promote prostate tumorigenesis via modulating androgen receptor-mediated CCL4-STAT3 signaling. *Cancer Res* 2013;73:5633-46.
 22. Streng T, Santti R, Talo A. Possible Action of the Proximal Rhabdosphincter Muscle in Micturition of the Adult Male Rat. *Neurourol Urodyn* 2001;20:197-210; discussion 210-3.
 23. Bernoulli J, Yatkin E, Laakso A, et al. Histopathological evidence for an association of inflammation with ductal pin-like lesions but not with ductal adenocarcinoma in the prostate of the noble rat. *Prostate* 2008;68:728-39.
 24. Yatkin E, Bernoulli J, Lammintausta R, et al. Fispemifene [Z-2-[2-[4-(4-chloro-1,2-diphenylbut-1-enyl)-phenoxy]ethoxy]-ethanol], a novel selective estrogen receptor modulator, attenuates glandular inflammation in an animal model of chronic nonbacterial prostatitis. *J Pharmacol Exp Ther* 2008;327:58-67.
 25. Lehtimäki J, Mäkelä S, Viljamaa J, et al. Neonatal Estrogenization of the Male Mouse Results in Urethral Dysfunction. *J Urol* 1996;156:2098-103.
 26. Streng T, Li X, Lehtoranta M, et al. Infravesical Obstruction in Aromatase Over Expressing Transgenic Male Mice With Increased Ratio of Serum Estrogen-To-Androgen Concentration. *J Urol* 2002;168:298-302.
 27. Streng TK, Talo A, Andersson KE, et al. A dose-dependent dual effect of oestrogen on voiding in the male mouse? *BJU Int* 2005;96:1126-30.
 28. Matsumoto S, Kawai Y, Oka M, et al. Bladder function in 17 b -estradiol-induced nonbacterial prostatitis model in Wistar rat. *Int Urol Nephrol* 2013;45:749-54.
 29. Dmochowski RR. Bladder Outlet Obstruction: Etiology and Evaluation. *Rev Urol* 2005;7:S3-13.
 30. Andersson KE, Arner A. Urinary Bladder Contraction and Relaxation : Physiology and Pathophysiology. *Physiol Rev* 2004;84:935-86.
 31. Levin RM, Haugaard N, O'Connor L, et al. Obstructive response of human bladder to BPH vs. rabbit bladder response to partial outlet obstruction: a direct comparison. *Neurourol Urodyn* 2000;19:609-29.
 32. Singh K, Sinha RJ, Sokhal A, et al. Does prostate size predict the urodynamic characteristics and clinical outcomes in benign prostate hyperplasia ? *Urol Ann* 2017;9:223-9.
 33. Taoka R, Kakehi Y. The influence of asymptomatic inflammatory prostatitis on the onset and progression of lower urinary tract symptoms in men with histologic benign prostatic hyperplasia. *Asian J Urol* 2017;4:158-63.
 34. Barros MH, Hauck F, Dreyer JH, et al. Macrophage polarisation: An immunohistochemical approach for identifying M1 and M2 macrophages. *PLoS One* 2013;8:e80908.
 35. Yamamichi F, Shigemura K, Arakawa S, et al. CD-163 correlated with symptoms (pain or discomfort) of prostatic inflammation. *Int J Clin Exp Pathol* 2015;8:2408-14.
 36. Hao NB, Lü MH, Fan YH, et al. Macrophages in Tumor Microenvironments and the Progression of Tumors. *Clin Dev Immunol* 2012;2012:948098.
 37. Yeh CR, Slavin S, Da J, et al. Estrogen receptor α in cancer associated fibroblasts suppresses prostate cancer invasion via reducing CCL5, IL6 and macrophage infiltration in the tumor microenvironment. *Molecular cancer* 2016;15:1-14.
 38. Keselman A, Fang X, White PB, et al. Estrogen Signaling Contributes to Sex Differences in Macrophage Polarization during Asthma. *J Immunol* 2017;199:1573-83.
 39. Penna G, Mondaini N, Amuchastegui S, et al. Seminal Plasma Cytokines and Chemokines in Prostate Inflammation: Interleukin 8 as a Predictive Biomarker in Chronic Prostatitis/Chronic Pelvic Pain Syndrome and Benign Prostatic Hyperplasia. *Eur Urol* 2007;51:524-33.
 40. Hajjghorbani M, Ahmadi-hamedani M, Shabab E, et al. Evaluation of the protective effect of pentoxifylline on carrageenan-induced chronic non-bacterial prostatitis in rats. *Inflammopharmacology* 2017;25:343-50.
 41. Hu C, Yang H, Yanfang Z, et al. The role of inflammatory cytokines and ERK1 / 2 signaling in chronic prostatitis/ chronic pelvic pain syndrome with related mental health disorders. *Sci Rep* 2016;6:28608.
 42. Said MM, Bosland MC. The anti-inflammatory effect of montelukast , a cysteinyl leukotriene receptor-1 antagonist , against estradiol-induced nonbacterial inflammation in the rat prostate. *Naunyn Schmiedebergs Arch Pharmacol* 2017;390:197-205.
 43. Montico F, Hetzl A, Candido E, et al. Angiogenic and tissue remodeling factors in the prostate of elderly rats submitted to hormonal replacement. *Anat Rec (Hoboken)*

- 2013;296:1758-67.
44. Motawi TK, Darwish HA, Diab I, et al. Combinatorial strategy of epigenetic and hormonal therapies: A novel promising approach for treating advanced prostate cancer. *Life Sci* 2018;198:71-8.
45. Watanobe H, Suda T. A detailed study on the role of sex steroid milieu in determining plasma leptin concentrations in adult male and female rats. *Biochemical and biophysical research communications* 1999;259:56-9.

Cite this article as: Konkol Y, Vuorikoski H, Streng T, Tuomela J, Bernoulli J. Characterization a model of prostatic diseases and obstructive voiding induced by sex hormone imbalance in the Wistar and Noble rats. *Transl Androl Urol* 2019;8(Suppl 1):S45-S57. doi: 10.21037/tau.2019.02.03